Non-communicating syringomyelia: a feature of spinal cord involvement in multiple sclerosis

Katrin Weier,[1] Yvonne Naegelin,[1] Alain Thoeni,[2] Jochen G. Hirsch,[2] Ludwig Kappos,[1] Wolfgang Steinbrich,[2] Ernst-Wilhelm Radue[2] and Achim Gass[1,2]

[1]Department of Neurology and [2]Department of Radiology/Neuroradiology, University Hospital Basel, Basel, Switzerland

Correspondence to: Achim Gass, MD, Department of Neurology/Neuroradiology, University Hospital Basel, Petersgraben 4, CH- 4031 Basel, Switzerland
E-mail: agass@uhbs.ch

In patients with multiple sclerosis (MS) non-communicating syringomyelia (NCS) has been described as an incidental finding in case studies and small case series. NCS in MS patients commonly leads to uncertainty particularly as the clinical picture of NCS is variable and surgical therapy may be considered. Up to date little is known about the prevalence and clinical importance of NCS in MS. We report the imaging and clinical characteristics of NCS formations in nine MS patients from a 1 year follow-up study in a representative group of 202 MS (4.5%) patients. Brain and spinal cord MRI was performed as part of a genetic study. NCS did commonly extend the central canal and the cord was slightly distended at the level of the syrinx. The cord and syrinx showed no tendency to change in size or shape over 1 year. Despite thorough search into the clinical history and current clinical status no definite but only minimal indications of symptoms potentially related to the NCS were found. We confirm that NCS may occur in MS patients with spinal cord pathology. It can be a subtle finding without clinical correlates. Syrinx formations are more likely to be a consequence of MS cord pathology than a coincidental finding.

Introduction

Syringomyelia describes a cavitary enlargement of the spinal cord, which may occur as one of three types (Milhorat *et al.*, 1995) (i) dilations of the central canal that communicate with the fourth ventricle; (ii) non-communicating dilations of the central canal that arise below a syrinx free segment of the cord and (iii) extracanalicular cavitations in the parenchyma that do not involve the central canal. The aetiology of syringomyelia is manifold and one can distinguish between symptomatic and congenital-idiopathic types. The latter is often associated with the Chiari malformations, basilar impression, Dandy-Walker cysts and sub-occipital encephalocele (Barnett *et al.*, 1973; Metcalfe, 1992; Anson *et al.*, 1997; Parker *et al.*, 1999). The symptomatic forms include intramedullary neoplasms and post-traumatic cavitations, which usually manifest some years after the cord injury (Reddy *et al.*, 1989). Furthermore, syrinx formations have been noted as a post-inflammatory phenomenon after basilar arachnoiditis (e.g. tuberculous meningitis), aseptic inflammatory processes or surgery (Barnett *et al.*, 1973; Caplan *et al.*, 1990).

In patients with multiple sclerosis (MS) non-communicating syringomyelia (NCS) has been described in various reports on small case series or case studies, one of them having access to a post-mortem analysis of pathological detail in the spinal cord (Kwee and Nakada, 1985; Ransohoff *et al.*, 1990; Milhorat *et al.*, 1992; Solaro *et al.*, 1999; Sotgiu *et al.*, 1999, 2001; Matsuda *et al.*, 2001; Charles *et al.*, 2004).

To date the relationship of NCS in MS and its prognosis is not well understood. The incidental finding of NCS is more common today with wider availability of whole cord MRI and leads usually to uncertainty particular as the clinical picture of NCS is variable and surgical therapy may be considered.

We had the opportunity to investigate the clinical and MRI characteristics of NCS in a follow-up study of a cohort of 202 MS patients as part of a phenotype-genotype study.

Methods and Materials

Patients

All patients included were participants in an ongoing study on the pheno-genotypic characterization of MS. A total of 259 MS patients (181 women, 78 men) were recruited from our MS out-patient clinic over 1 year. Of those patients, 202 (140 women, 62 men; 20- to 67-years-old) had complete MRI assessment including brain and spinal cord MRI at baseline and at year 1. The remaining 50 patients were not included for the lack of the complete MRI assessment. At the time, all patients were assessed clinically with a standardized neurological examination and a comprehensive disease history. At the time of the follow-up visit 12 months after baseline NCS was known and the clinical history and neurological examination focused on potential clinical manifestations of NCS (e.g. pain syndromes, dissociated sensory loss). Of the 202 patients, 147 had relapsing-remitting MS (RRMS) disease course, 39 secondary progressive MS (SPMS) and 10 primary progressive MS (PPMS). Six patients had the diagnosis of a clinically isolated syndrome (CIS). The mean disease duration was 14 years, the Expanded Disability Status Scale (EDSS) ranged from 0 to 7.5. All patients were clinically stable. Patients having an acute relapse were not examined and the MRI scan was postponed at least 30 days after the last dose of steroid treatment. Informed consent was obtained in writing from all participating patients, in accordance with the institution's medical ethics committee approval. In the nine patients with a syrinx an additional laboratory test for anti-aquaporin-4 antibodies was performed to test for neuromyelitis optica.

MRI

Brain and cord MRI was obtained in a single examination on a 1.5T MRI system, MAGNETOM Avanto (Siemens Medical Solutions, Erlangen, Germany). The brain MRI protocol included transverse 3 mm proton density (PD)-weighted, T_2-weighted and T_1-weighted sequences before and after single dose gadolinium application.

The spinal cord scan took place immediately after brain MRI within the same scanning session. The delay between a single dose gadolinium contrast injection for the brain MRI and the acquisition of sagittal images was ∼10 min. For theoretical reasons, the previous injection of the contrast agent might have shortened the transverse relaxation time in pathology and thereby reduced the sensitivity of PD- and T_2-weighed sequences. This was not observed in previous and subsequent diagnostic examinations, when this potential influence was considered in particular. In order to cover the large area of the whole spinal canal from the foramen magnum to the sacral vertebrae two separate sets of images were generated with two FOVs of $350 \times 350\,mm^2$ size (including 50% phase oversampling in head–feet direction to avoid aliasing), the top part showing the cranio-cervical junction up to the 9th thoracic vertebral body and the caudal set of images covering the spine from 9th thoracic vertebra downwards to the first sacral vertebra. In a post-processing step on the console by manufacturer provided software, the two sagittal images were distortion corrected and fused to demonstrate the whole spine.

Sagittal and transverse PD- and T_2-weighted turbo-spin-echo sequences were acquired with multi-array-coils and parallel imaging techniques. Two sagittal sequences with PD [TR/TE 2000 ms/23 ms, echo train length (ETL) 7, iPAT-factor 2, two averages, acquisition time (TA) 2:40 min] and T_2-weighting (TR/TE 4440 ms/102 ms, ETL 25, iPAT 2, TA 2 : 32 min) were obtained, with two overlapping FOVs
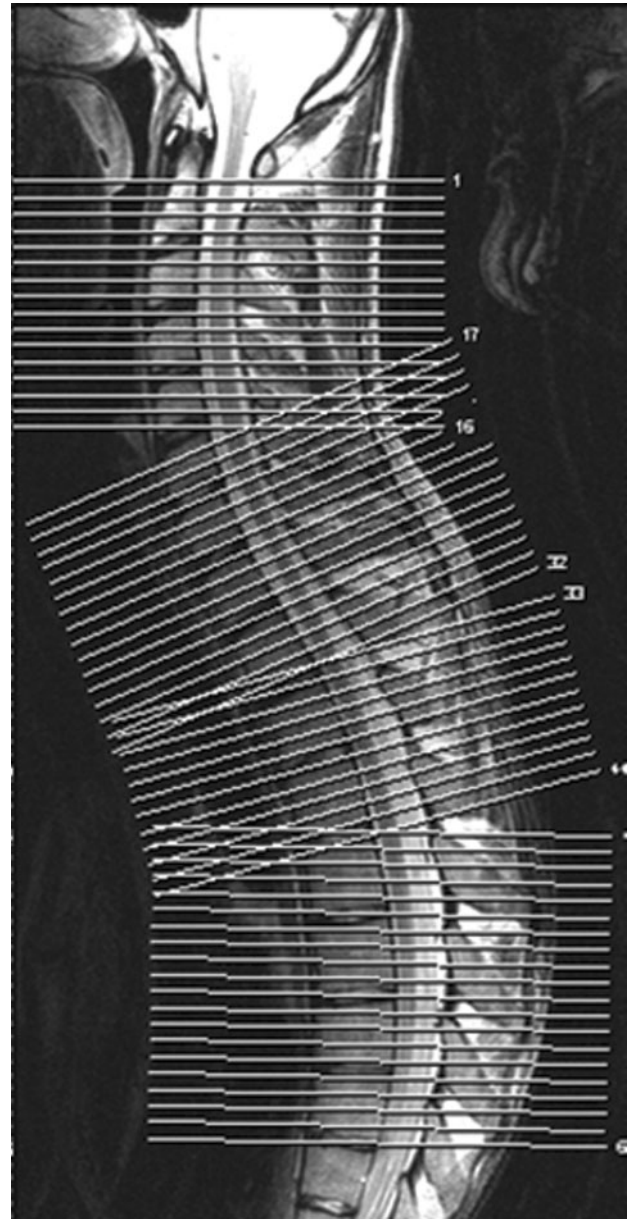

Fig. 1 Sagittal T_2-weighted image of the spinal cord showing graphical planning of transverse slices covering the whole cord. Four stacks of slices are placed perpendicular to the cord at the respective levels.

of $350 \times 350\,mm^2$ resulting in a voxel size of $1.0 \times 0.8 \times 3\,mm$. Subsequently, two sets of 60 transverse 6 mm PD-/T_2-weighted slices of the entire spinal cord were acquired using a dual-echo turbo-spin-echo sequence: TR/TE1/TE2 2120/9.9/89 ms, 2 NEX, ETL 7, iPAT 2, $1.1 \times 0.5 \times 6\,mm$ resolution, TA 4:51 min. The transverse slices were prescribed graphically in a standardized way (Fig. 1): four stacks, each with 12–19 transverse slices were placed perpendicular to the cord manually adjusted along the anatomic course of the cord from the foramen magnum to the conus of the SC. The parallel imaging factor was 2 for the above sequences. The total acquisition time of the whole spinal cord in two planes was ∼11 min.

The patients in whom a syrinx was identified underwent an additional sagittal pre-contrast and a sagittal (TR/TE 676 ms/13 ms) and transverse post-contrast (single dose gadoterate meglumine)

Fig. 2 T$_2$-weighted images of the nine MS patients with syringomyelia in sagittal and transverse perspective. Syrinx formations vary in length and cross-sectional diameter, some show a slightly distending effect on the cord.

T$_1$-weighted scan (TR/TE 684 ms/11 ms) in order to exclude further abnormalities.

Data analysis

A standardized qualitative reporting scheme for the presence and location of intrinsic cord changes (e.g. focal lesions, diffuse changes, atrophy) and other pathology was employed by a consensus reading of two experienced readers. In the nine patients with a syrinx formation, previous medical charts and MRI (when available) were also considered. Digital images of those patients were further analysed on a dedicated Siemens work station.

Results

MRI analysis identified in 9/202 (4.5%) MS patients syrinx formations in the spinal cord (Fig. 2). Digital quantitative analysis results are given in Table 2.

Clinical findings (Table 1)

A diagnosis of MS had been established including positive oligoclonal bands on CSF analysis. Patients presented with a wide range of symptoms and mean EDSS was 2.6 (0–6.5). Careful clinical examination showed in none of the cases dissociated sensory loss, a typical pain syndrome or suggested a focal functional deficit arising from the area of the syrinx level. Please see Table 2 for patient data. Patient 7 had been diagnosed with MS 8 years earlier and had undergone hemilaminectomy at the level of the 5th lumbar vertebral body for radicular decompression after disc protrusion and sensory-motor disturbance. A syrinx like formation was found in this patient in the thoracic cord at the level of the 8th thoracic vertebral body. In none of the patients a previous history of trauma, cord surgery, or previous intervention besides the lumbar puncture for diagnostic CSF analysis were identified. Acute relapses were noted in 3/9 patients in the 12 month prior to the baseline scan. In 5/9 patients an acute relapse was recorded in the 12 month interval between baseline and follow-up MRI.

All acute relapse symptoms subsided and no permanent change of the EDSS was present at the clinical 12 month follow-up assessment. The nine patients with a syrinx were negative for anti-aquaporin-4 antibodies.

MRI (Fig. 2, Table 2)

In nine MS patients with syrinx formations in the spinal cord, the brain MRI demonstrated typical MS brain lesions, while patients 2 and 7 showed only 1, respectively, 4 brain lesions. There was no overt brain atrophy or pathological contrast enhancement. Proton density- and T$_2$-weighted spinal cord MRI demonstrated evidence of focal hyperintense lesions, but no diffuse T$_2$-hyperintense abnormalities or atrophic cord changes. Five patients showed slight degenerative changes of the vertebral column, but not causing cord compression or relevant narrowing of the CSF space. None of the patients showed abnormalities of the cranio-cervical junction or indications for abnormality within the CSF space. The syrinx formations were located either in the thoracic or lumbar cord (Fig. 3). The cross-sectional location of the syrinx appeared to be in the position of the central canal as interpreted from the sagittal and transverse images in all cases. One patient showed three non-communicating cavitations at different levels of the cord separated by syrinx-free segments, while 8/9 had a single syrinx. The extension of each cavity ranged from less than one vertebral body up to more than five vertebral bodies (2.5–17 cm length). The cavity diameter ranged from 15 to 50 mm. On sagittal images the cord appeared slightly distended in patients 1–3 and more pronounced so in patients 4–9.

Concomitant MS cord lesions were present in all patients. While patient 2 had only one lesion below the syrinx, the other patients had lesions above the syrinx whilst both lesions above and below the syrinx were noted in three patients (6, 8 and 9). In three patients (1, 7 and 9) cord lesions were present in proximity to the syrinx, close to the cranial (1, 7) or caudal end of the syrinx. There was

Table 1 Demographic and clinical information of the nine MS patients with syrinx formations

Patient no.	1	2	3	4	5	6	7	8	9
Sex/age (years)	m, 38	w, 35	m, 45	w, 36	w, 55	m, 54	w, 61	w, 56	w,34
Disease course	RRMS	RRMS	RRMS	RRMS	RRMS	SPMS	SPMS	RRMS	RRMS
Disease duration (years)	3	8	7	14	8	28	8	8	14
CSF oligoclonal bands	Positive	Positive	Positive	Positive	Positive	Positive	Positive	Positive	Positive
Anti-aquaporin-4-antibody titer	Negative	Negative	Negative	Negative	Negative	Negative	Negative	Negative	Negative
Presenting symptoms	Hypaesthesia left buttock, hip and thigh	Hypaesthesia left sided trunk + leg	Weakness left leg, urgency	Paraesthesia in all limbs, weakness left arm	Urgency	Diplopia	Hypesthesia both hands	Diplopia	Paraesthesia of both legs
Subsequent symptoms (potentially cord related)	Slight urgency	–	Hypaesthesia leg, transient weakness right leg	Slight weakness of left limbs, dysaesthesia left trunk	Slight weakness left leg	Progressive spastic tetraparesis	Frequent urinary tract infection, retention	Slight spasticity of left leg gait, transient weakness right leg	Transient dys- and hypaesthesia below the level of thoracic dermatome 4
Current symptoms (potentially cord related)	No symptoms	No symptoms	Slight urgency, imbalance	No symptoms	Motor and cognitive fatigability, urgency	spastic tetraparesis, urgency	Paraesthesias both hands, fatigability, urgency	Weakness right arm + leg, motor fatigability, urgency	no symptoms
Current findings (potentially cord related)	No Sc-symptoms	No Sc-symptoms	Bilateral pallhypaesthesia	No Sc-symptoms	Pyramidal weakness of both legs, bilateral pallhypaesthesia, urgency, retention	spastic tetraparesis	Bilateral pallhypaesthesia	Motor fatigability, pallhypaesthesia	Bilateral pallhypaesthesia
No. of relapses 12 month prior to first scan	–	–	–	1	–	–	–	1	2
No. of relapses between baseline and fu scan	1	1	2	1	–	–	–	2	–
EDSS	0	1.5	2	2.5	3	6.5	2.5	4	1.5
Current therapy	Interferon β-1a	Glatiramer acetate	Interferon β-1a	Interferon β-1b	Interferon β-1a	–	Interferon β-1b	Interferon β-1b	Interferon β-1a

Table 2 MR findings in nine patients with syrinx formations

Patient no.	1*	2	3	4	5	6	7	8	9
Size in length (cm)	A: 4; B: 3; C: 10.5	2.5	9	3.5	3.5	17	15	4.5	4.5
Location according to the level of vertebral bodies**	A: TH 4/5; B: TH 7/8; C: TH 9 – L1	TH 3/4	TH 5–9	TH 5/6	TH 6/7	TH 5–10	TH 8–L1	TH 8–9	TH 5–7
Maximum cross-sectional area of the syrinx (mm^2)	A: 2.3; B: 2.6; C: 8.4	28.3	9.8	4.6	2.0	4.6	4.9	3.5	3.2
Cord cross-section above the syrinx (mm^2)	A: 58.3; B: 52.8; C: 54.2	44.7	43.6	44.7	41.3	51.6	49.3	39.8	40.1
Cord cross-section at the level of the syrinx (mm^2)	A: 55.4; B: 49.9; C: 71.8	128.1	56.8	52.5	44.7	48.2	57.7	43.0	49.3
MS lesions in the proximity to the syrinx according to:									
a) the top of the syrinx	–	–	–	–	–	–	1	–	–
b) the level of the syrinx	1	–	–	–	–	–	–	–	1
c) the bottom of the syrinx	–	–	–	–	–	–	–	–	1
Additional cord changes (acc. to the level of vertebral bodies**)									
No. of focal lesions (total)	6	–	4	3	3	8	1	5	5
a) cervical	5	–	3	3	3	5	1	4	3
b) thoracic	1	–	1	–	–	3	–	1	2
Diffuse T$_2$-hyperintensities	–	–	–	–	–	–	–	–	–
Changes of the syrinx formation after 1 year f/u	No	No	No	No	No	No	No	No	No
Brain									
T$_2$ lesion volume (mm^3)	826	40	2552	15 356	17 170	4020	14	6145	337
T$_1$ volume (mm^3)	171	0	512	4523	3070	1948	0	2160	103
No. of Gd+ lesions***	0	0	0	0	0	0	0	0	0

*Pat. No. 1 shows three separate syrinx formations at different cord levels. **TH = thoracic vertebral body; L = lumbar vertebral body.
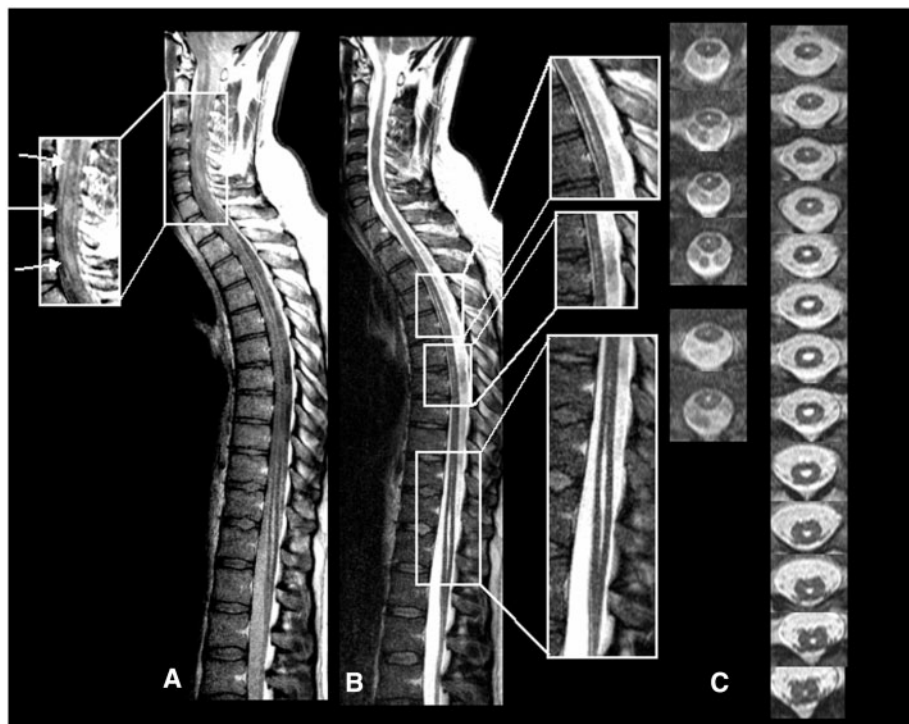***Gd+ = contrast enhancement (Dotarem®).

Fig. 3 Sagittal and transverse PD- (**A**) and T$_2$-weighted (**B**) images of the entire cord of patient 1. Three focal lesions (arrows) in the cervical cord are more strongly contrasted on PD images (**A**) (see magnification on the left) whereas the syrinx formations at the thoracic and lumbar levels are more strongly contrasted on the T$_2$-weighted images (**B**). The transverse plane (**C**) demonstrates the location of the syrinx in relation to cord cross-section.

no uniform pattern in regard to the size or cross-sectional location of those lesions.

The additional pre- and post-contrast T_1-weighted MRI, which was only performed in the nine patients with the syrinx, did not show pathological contrast enhancement or any additional pathology. Compared with the T_2-weighted images it was more difficult to acertain the small hypo-intense syrinx on the T_1-weighted images due to the lower contrast between cord tissue and syrinx.

Follow-up spinal cord MRI after 1 year in all cases demon-strated no change of the MR appearance of the above described cord findings. Both the previous history and the follow-up MRI revealed no indication of cord neoplasms.

Discussion

Syrinx formations in MS patients have been described previously in case reports as incidental findings. This study offers a broad view at NCS in MS patients by examining a relatively large representative cohort with a wide range of clinical characteristics, who were originally recruited for a genetic study to represent a wide spectrum of MS. As demonstrated by MRI, the size of syrinx formations is variable and frequently NCS is a rather subtle finding, but the technology used in this study (parallel imaging in combination with multi-array-coils) allowed to ascertain the NCS by using T_2-weighted sequences in two imaging planes (Noebauer-Huhmann *et al.*, 2007). While truncation artefact is a common source of high signal bands on sagittal T_2-weighted images (Taber *et al.*, 1998) that can obscure a syrinx pathology the presence of NCS was confirmed on the axial cord MRI in this study.

We found NCS in 4.5% of our MS cohort. Compared with this data estimations of the prevalence of NCS in the normal population are very difficult. In a study of the whole cord Thorpe and colleagues did not find any intrinsic cord abnormality in 50 normal controls (Thorpe *et al.*, 1993), which is very much the experience from diagnostic MRI in patients investigated for degenerative disc disease. Given the potential lack of obvious clinical symptoms related to the syrinx, one may assume that syringomyelia may remain undetected in healthy individuals. However, in epidemiological studies the prevalence of syringomyelia ranges from 8.4/100 000 to 0.9/10 000 (Brewis *et al.*, 1966; Ferrero Arias and Pilo Martin, 1991). In MS patients, demyelinating lesions of the cord regularly show some evolution over time, however, the NCS formations in this study were unchanged in all cases over the 1 year follow-up period. In two patients, who had undergone previous spinal MRI exams, NCS was stable even over 5 years follow-up. In this regard, the syrinx was not a transient phenomenon but a rather stable MR finding and its frequency in our cohort may be useful to estimate the prevalence in MS.

The nine patients with syrinx formations had relapsing forms of MS with variable disease durations ranging from early RRMS to SPMS with superimposed relapses. There were no peculiar clinical histories or uncommon clinical findings suggesting another differential diagnosis or a second pathol-ogy. In particular, neuromyelitis optica (NMO) needs to be considered in patients with an uncommon cord pathology and a diagnosis of inflammatory-demyelinating disease. However, our patients all were initially diagnosed with MS and they were negative for anti-aquaporin-4 antibodies. In the absence of both anti-aquaporin-4 antibodies and typical extensive multilevel cord lesions it appears not likely that the patients were initially misdiagnosed and NMO was the underlying cause. So far clinical and radiological descriptions of NMO do not include a syrinx as an early or late finding. Furthermore, common causes of syringomyelia were excluded and there were no indications of cord neoplasm. In contrast to some previous case reports, our patients were either asymp-tomatic or not obviously clinically affected by the NCS. Patients 3, and 5–9 showed symptoms possibly due to spinal cord lesions but no typical clinical presentations of syringo-myelia. However, a contribution of the syrinx to the clinical presentations would be very difficult to exclude. In keeping with our findings, a recent literature review pointed out, that in most reported cases syringomyelia has been an incidental finding when patients underwent MRI not for clinically suspected syrinx but spinal cord involvement of MS (Larner *et al.*, 2002).

We assume that NCS is not a coincidental finding but associated with spinal cord involvement in MS. The lower prevalence of NCS in the normal population speaks in favour of a causal relationship of inflammatory-demyelinating pathology and NCS. This being said, NCS did not appear to be strictly related to some specific location or detectable cross-sectional topographical relationship to demyelinating cord lesions. Most MS lesions in our patients were found in the cervical cord, but the NCS were located in the thoracic or lumbar cord. As reviewed in recent papers the fluid accu-mulation in the syrinx probably represents lack of physiolo-gical CSF drainage in the central canal (Ball and Dayan, 1972; Milhorat *et al.*, 1994; Kleinschmidt-DeMasters and Newell, 1996). Residual CSF signal can be observed regularly in the position of the central canal in the normal cord. The mecha-nism for the formation of a syrinx in MS patients is uncertain, but one could hypothesize, that residual cord tissue changes might alter normal CSF drainage from the central canal. However, there was no uniform spatial relationship of cord lesions to the NCS that could confirm such a hypothesis. We conclude that, in the presence of other cord and brain lesions typical for MS, a syrinx can be due to MS. However, as long as the exact mechanism of the development of such small cavities is uncertain other causes should be considered.

Acknowledgements

References

Anson JA, Benzel EC, Awad IA, editors. Syringomyelia and the Chiari malformations. Park Ridge, IL: American Association of Neurological Surgeons, 1997.

Ball MJ, Dayan AD. Pathogenesis of syringomyelia. Lancet 1972; 2: 799–801.

Barnett HJM, Foster JB, Hudgson P. Syringomyelia. London: WB Saunders, 1973.

Brewis M, Poskanzer DC, Rolland C, Miller H. Neurological diseases in an English city. Acta Neurol Scand 1966; 42 (Suppl 24): 1–89.

Caplan LR, Norohna AB, Amico LL. Syringomyelia and arachnoiditis. J Neurol Neurosurg Psychiatry 1990; 53: 106–13.

Charles JA, Berger M, Cook SD. Thoracic syringomyelia and suspected multiple sclerosis: cause and effect or coincidence? Neurology 2004; 63: 185–6.

Ferrero Arias J, Pilo Martin I. Prevalence of several neurological diseases in the central provinces of the Iberian Peninsula in eighteen-year-old males. Neurologia 1991; 6: 89–94.

Kleinschmidt-DeMasters BK, Newell J. Multiple sclerosis with hydromyelia demonstrated at autopsy. J Neurol Sci 1996; 136: 185–8.

Kwee IL, Nakada T. Syrinx formation in multiple sclerosis. Br J Radiol 1985; 58: 1206–8.

Larner AJ, Muqit MM, Glickman S. Concurrent syrinx and inflammatory central nervous system disease detected by magnetic resonance imaging: an illustrative case and review of the literature. Medicine 2002; 81: 41–50.

Matsuda M, Tabata K, Miki J, Ishigame H, Asano M, Ikeda S. Multiple sclerosis with secondary syringomyelia. An autopsy report. J Neurol Sci 2001; 184: 189–96.

Metcalfe R. Craniocervical anomalies and non-traumatic syringomyelia. In: Critchley E., Eisen A, editors. Diseases of the spinal cord. London: Springer-Verlag, 1992. p. 181–200.

Milhorat TH, Capocelli AL Jr., Anzil AP, Kotzen RM, Milhorat RH. Pathological basis of spinal cord cavitation in syringomyelia: analysis of 105 autopsy cases. J Neurosurg 1995; 82: 802–12.

Milhorat TH, Johnson WD, Miller JI, Bergland RM, Hollenberg-Sher J. Surgical treatment of syringomyelia based on magnetic resonance imaging criteria. Neurosurgery 1992; 31: 231–44; discussion 244–5.

Milhorat TH, Kotzen RM, Anzil AP. Stenosis of central canal of spinal cord in man: incidence and pathological findings in 232 autopsy cases. J Neurosurg 1994; 80: 716–22.

Noebauer-Huhmann IM, Glaser C, Dietrich O, Wallner CP, Klinger W, Imhof H, et al. MR imaging of the cervical spine: assessment of image quality with parallel imaging compared to non-accelerated MR measurements. Eur Radiol 2007; 17: 1147–55.

Parker F, Aghakhani N, Tadie M. [Non-traumatic arachnoiditis and syringomyelia. A series of 32 cases]. Neurochirurgie 1999; 45 (Suppl 1): 67–83.

Ransohoff RM, Whitman GJ, Weinstein MA. Noncommunicating syringomyelia in multiple sclerosis: detection by magnetic resonance imaging. Neurology 1990; 40: 718–21.

Reddy KK, Del Bigio MR, Sutherland GR. Ultrastructure of the human posttraumatic syrinx. J Neurosurg 1989; 71: 239–43.

Solaro C, Uccelli A, Gentile R, Lentino C, Mancardi GL, Primavera A. Multiple sclerosis and non-communicating syringomyelia: a casual association or linked diseases? Acta Neurol Scand 1999; 100: 270–3.

Sotgiu S, Pugliatti M, Rosati G, Sechi GP. Which syringomyelia is truly associated with multiple sclerosis? J Neurol Sci 2001; 190: 99–100.

Sotgiu S, Sechi G, Pugliatti M, Valenti P, Rosati G, Achene A, et al. Multiple sclerosis associated with syringomyelia. J Neurol Neurosurg Psychiatry 1999; 67: 248.

Taber KH, Herrick RC, Weathers SW, Kumar AJ, Schomer DF, Hayman LA. Pitfalls and artifacts encountered in clinical MR imaging of the spine. Radiographics 1998; 18: 1499–521.

Thorpe JW, Kidd D, Kendall BE, Tofts PS, Barker GJ, Thompson AJ, et al. Spinal cord MRI using multi-array coils and fast spin echo. I. Technical aspects and findings in healthy adults. Neurology 1993; 43: 2625–31.